Title

SARS-CoV-2 Serology Across Scales: A Framework for Unbiased Estimation of Cumulative Incidence Incorporating Antibody Kinetics and Epidemic Recency.

Authors

Takahashi, Saki
Peluso, Michael
Hakim, Jill
et al.

Practice of Epidemiology

SARS-CoV-2 Serology Across Scales: A Framework for Unbiased Estimation of Cumulative Incidence Incorporating Antibody Kinetics and Epidemic Recency

Saki Takahashi*, Michael J. Peluso, Jill Hakim, Keirstinne Turcios, Owen Janson, Isobel Routledge, Michael P. Busch, Rebecca Hoh, Viva Tai, J. Daniel Kelly, Jeffrey N. Martin, Steven G. Deeks, Timothy J. Henrich, Bryan Greenhouse, and Isabel Rodríguez-Barraquer

* Correspondence to Dr. Saki Takahashi, Department of Epidemiology, Johns Hopkins Bloomberg School of Public Health, Baltimore, MD 21205 (e-mail: saki.takahashi@jhu.edu).

Serosurveys are a key resource for measuring severe acute respiratory syndrome coronavirus 2 (SARS-CoV-2) population exposure. A growing body of evidence suggests that asymptomatic and mild infections (together making up over 95% of all infections) are associated with lower antibody titers than severe infections. Antibody levels also peak a few weeks after infection and decay gradually. We developed a statistical approach to produce estimates of cumulative incidence from raw seroprevalence survey results that account for these sources of spectrum bias. We incorporate data on antibody responses on multiple assays from a postinfection longitudinal cohort, along with epidemic time series to account for the timing of a serosurvey relative to how recently individuals may have been infected. We applied this method to produce estimates of cumulative incidence from 5 large-scale SARS-CoV-2 serosurveys across different settings and study designs. We identified substantial differences between raw seroprevalence and cumulative incidence of over 2-fold in the results of some surveys, and we provide a tool for practitioners to generate cumulative incidence estimates with preset or custom parameter values. While unprecedented efforts have been launched to generate SARS-CoV-2 seroprevalence estimates over this past year, interpretation of results from these studies requires properly accounting for both population-level epidemiologic context and individual-level immune dynamics.

cumulative incidence; SARS-CoV-2; seroepidemiology; seroprevalence; spectrum bias

Abbreviations: CrI, credible interval; PCR, polymerase chain reaction; SARS-CoV-2, severe acute respiratory syndrome coronavirus 2.

Numerous severe acute respiratory syndrome coronavirus 2 (SARS-CoV-2) seroprevalence surveys ("serosurveys") have been conducted to measure population exposure to this novel pathogen (1, 2). The need to consider basic assay performance characteristics (i.e., sensitivity and specificity) to accurately estimate seroprevalence (i.e., the proportion of the population that has antibodies) has been well-established (3–5). Accurate estimation of cumulative incidence (i.e., the proportion of the population that has ever experienced infection) relies on adequate characterization of assay sensitivity to detect prior infections in the general population. However, for most commercially available assays, manufacturer-reported performance characteristics are usually applicable only to early convalescent samples from hospitalized patients; notably, antibody responses in these individuals are not representative of antibody responses in the general population. Sufficiently accounting for SARS-CoV-2 antibody responses varying as a function of disease severity (6, 7) and waning over time (8, 9) is necessary to correctly estimate cumulative incidence from serosurveys performed using these assays.

Relying on validation samples that do not represent the spectrum or distribution of severity and time since infection in a study population can introduce what is commonly known as "spectrum bias" into cumulative incidence estimation, whereby assay performance characteristics determined from the validation samples do not reflect assay performance in the study population (10, 11). Various modeling
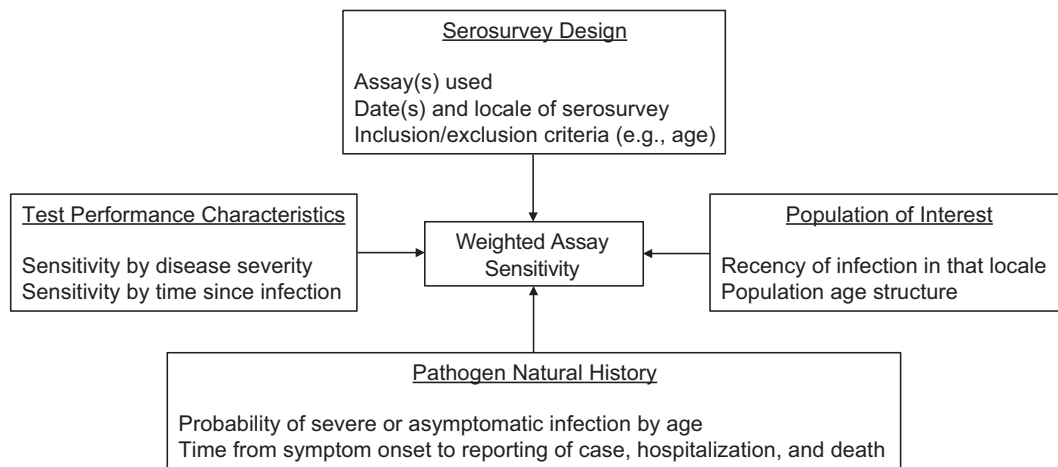
Figure 1. Schematic of the cumulative-incidence estimation framework for unbiased estimation of cumulative incidence. Each of the 4 boxes on the perimeter details its contributions to the target output of weighted assay sensitivity (center).

approaches have been proposed to reduce the effects of spectrum bias stemming from antibody waning over time and seroreversion on serological platforms (12–16). A key advance of our approach is the ability to parametrize seroreversion using longitudinal antibody kinetic data generated from the same assays used in large-scale serosurveys. To our knowledge, differential antibody responses by disease severity (and factors associated with severity such as age (17)) have not yet been incorporated alongside these temporal considerations into a unified framework to accurately estimate cumulative incidence from serosurveys. Failing to account for factors that reduce assay sensitivity will typically underestimate the cumulative incidence of SARS-CoV-2 in the population (11).

We present a flexible statistical approach to produce cumulative incidence estimates from seroprevalence data, considering assay-specific test performance characteristics by severity and time (Figure 1). To inform parametrization of the magnitude and kinetics of SARS-CoV-2 immune responses, we used data from a postinfection cohort study with some of the commercial serological platforms that have been most widely used throughout the pandemic (18). We applied this approach to reanalyze large-scale serosurveys from 5 locales: Italy, Spain, the United States, Manaus (Brazil), and Japan. Broadly, incorporating variability in individual-level immune dynamics into population-level epidemiologic estimates allows for more accurate estimation of cumulative incidence, which opens the way for more accurate characterization of population exposure, transmission dynamics, and infection-fatality ratios.

METHODS

Estimating time-varying, severity-specific assay sensitivities

To estimate time-varying, severity-specific assay sensitivities (i.e., the probability of testing positive in a serosurvey, given prior infection), we used longitudinal antibody

response data collected from a cohort of participants with polymerase chain reaction (PCR)-confirmed SARS-CoV-2 through the University of California, San Francisco–based Long-term Impact of Infection with Novel Coronavirus (LIINC) natural history study (NCT04357821). Extensive descriptions of the cohort and laboratory results, including antibody responses on 14 commercial and research-use assays, are available elsewhere (18–20). Briefly, we reanalyzed data published in Peluso et al. (18) to estimate assay sensitivity as a function of disease severity and time since symptom onset (Web Table 1, available at https://doi.org/10.1093/aje/kwad106). As in Peluso et al. (18), we calibrated the time metric from days since symptom onset (or days since positive PCR test, for asymptomatic individuals) to days since expected seroconversion by adding 21 days to the former (21). For parsimony, we equated having had severe disease with having required hospitalization (17, 22).

Building off of the approach in Peluso et al. (18), individuals were partitioned into 2 severity groups depending on whether they were hospitalized for their SARS-CoV-2 infection. We modeled log-transformed signal-to-cutoff (S/C) or cutoff-index (COI) values using Bayesian linear mixed-effects models (Figure 2; see Web Appendix 1) (23). We estimated sensitivity by severity group and assay continuously for up to 1 year following expected seroconversion (Web Table 2). In sensitivity analyses, we further partitioned nonhospitalized individuals into separate severity groups by asymptomatic and symptomatic. We also extended these methods to estimate bivariate test performance characteristics from data where every sample was tested on two assays for which results may be correlated (see Web Appendix 2).

SARS-CoV-2 serosurveys included for application of adjustment framework

The published large-scale serosurveys reanalyzed here were conducted in 5 locales (24–31). As outlined in Table 1, multiple differences exist between these serosurveys in

Table 1.   SARS-CoV-2 Population Serosurveys Included From Italy, Spain, United States, Manaus (Brazil), and Japan, 2020–2021

Serosurvey (Sample Size)	Serosurvey Rounds Included in This Analysis	Assays Used and Included in This Analysis	Study Design and Population	Spatial Resolution of Results	Age-Stratification of Results	Sex-Stratification of Results	Reported Seroprevalence	Reference
Italy (64,660)	May 25 through July 15, 2020	Abbott ARCHITECT	Population-based	Region[a]	No[b]	No[b]	2.5%	(24, 53; Figure 1)
Spain (round 1: 55,004; round 2: 56,138)	Round 1: April 27 through May 11, 2020; round 2: May 18 through June 1, 2020	Abbott ARCHITECT	Population-based	Province[c]	No[d]	No[d]	Round 1: 5.0%[e]; round 2: 5.2%[e]	(25, Figure 4; 26, 27)
United States (177,919 total in 4 rounds)[f]	Round 1: July 27 through August 13, 2020; round 2: August 10–27, 2020; round 3: August 24 through September 10, 2020; round 4: September 7–24, 2020	Abbott ARCHITECT, Roche Elecsys, or Ortho VITROS IgG[g]	Residual samples from commercial laboratories	US census division[h]	Years: 0-17; 18–49; 50-64; ≥65	Yes	Various	(28, 40)
Manaus, Brazil (9,839 total in 10 rounds)[i]	10 monthly cross-sections from April 2020 through January 2021	Abbott ARCHITECT	Blood donors	Single city	Years: 15–24; 25–34; 35–44; 45–54; 55–64; 65–70	Yes	Various	(29, 30)
Japan (15,043)	December 14-25, 2020	Abbott ARCHITECT and Roche Elecsys[j]	Convenience sampling	Prefecture[k]	N/A[l]	No	Tokyo: 0.91%[m]; Osaka: 0.58%[m]; Miyagi: 0.14%[m]; Aichi: 0.54%[m]; Fukuoka: 0.19%[m]	(31)

Abbreviations: N/A, not available; SARS-CoV-2, severe acute respiratory syndrome coronavirus 2.

[a] 21 regions total.

[b] Population-based serosurvey designed to be representative.

[c] 52 provinces total.

[d] Population-based serosurvey designed to be representative.

[e] Based on Orient Gene Biotech (Huzhou, Zhejiang, China) COVID-19 IgG/IgM rapid test; not reported for Abbott (Abbott Park, Illinois) ARCHITECT assay.

[f] 177,785 included in analysis; removed 132 data points missing age and 4 samples missing sex; mean: 44,480 per round.

[g] Each sample was tested on one of these 3 assays: Abbott ARCHITECT, Roche Elecsys (Indianapolis, Indiana), or Ortho VITROS IgG (Raritan, New Jersey).

[h] 9 census divisions total: Pacific, Mountain, West North Central, East North Central, West South Central, East South Central, Middle Atlantic, New England, and South Atlantic and Puerto Rico.

[i] 9,838 included in analysis; removed 1 data point under 15 years of age; mean: 984 per round.

[j] Parallel testing of all samples on both the Abbott ARCHITECT and Roche Elecsys assays.

[k] 47 prefectures total; 5 included in analysis: Tokyo, Osaka, Miyagi, Aichi, and Fukuoka prefectures.

[l] Inclusion criteria of ≥20 years.

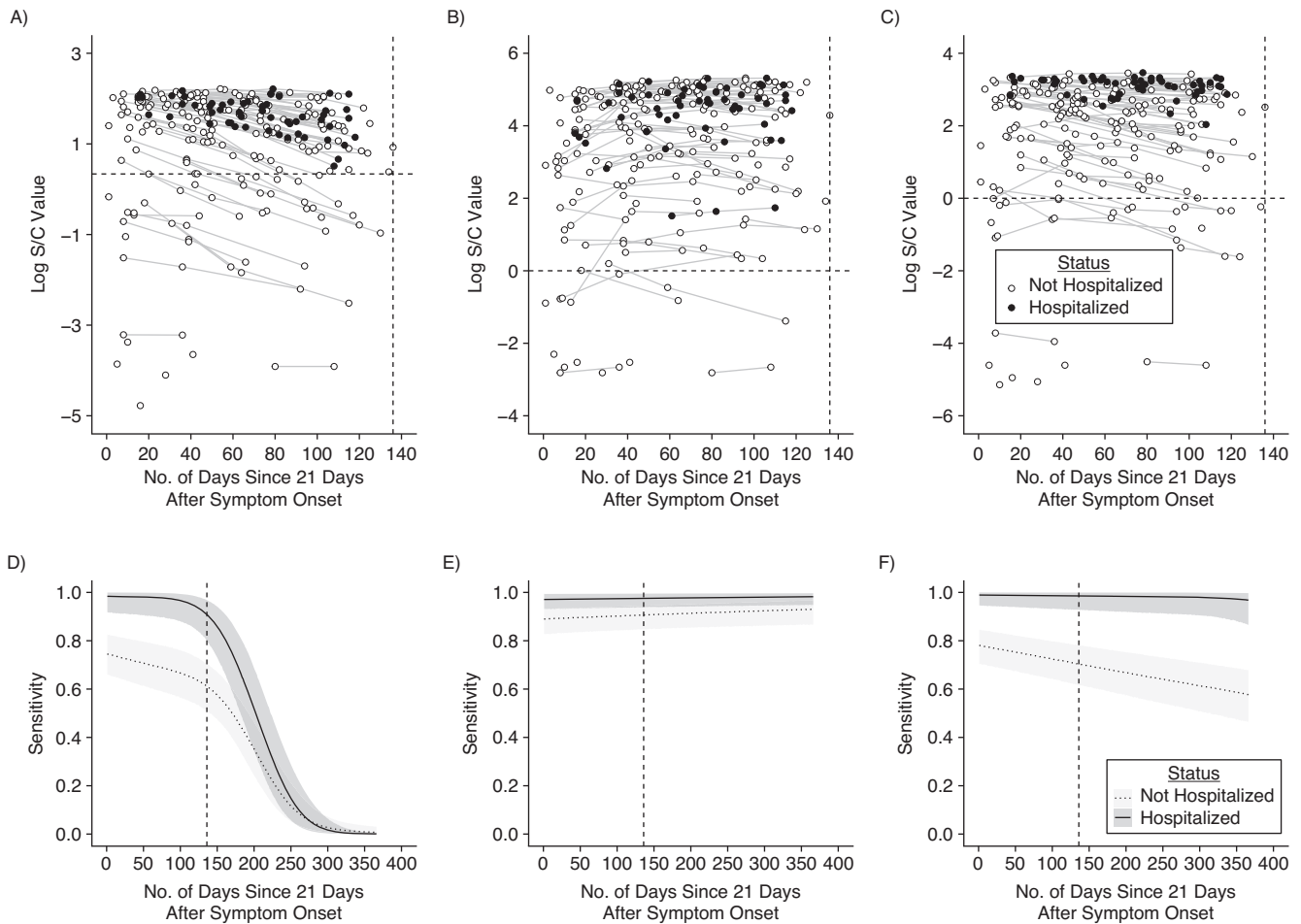[m] Based on positive test result on both assays.

Figure 2. Longitudinal severe acute respiratory syndrome coronavirus 2 (SARS-CoV-2) antibody kinetics and estimated assay sensitivities according to time and hospitalization status. Days since symptom onset (offset by 21 days) is shown on the *x*-axis versus the log-transformed antibody response for each of the Abbott (Abbott Park, Illinois) ARCHITECT (A), Roche (Indianapolis, Indiana) Elecsys (B), and Ortho (Raritan, New Jersey) VITROS IgG (C) assays, stratified by hospitalization status (empty circle indicates nonhospitalized; filled circle indicates hospitalized). For asymptomatic individuals, the time since the first positive PCR test (offset by 21 days) was used. This time metric is referred to as "time since seroconversion" hereafter. Longitudinal samples are connected by thin lines. The dashed horizontal line indicates the cutoff value for positivity on that assay. The dashed vertical line indicates the maximum observed time (*x* = 136 days). The key is shared across panels A–C. Estimated sensitivity for each of the Abbott ARCHITECT (D), Roche Elecsys (E), and Ortho VITROS IgG (F) assays (showing posterior median estimates and 95% credible intervals), stratified by hospitalization status (light gray with dotted line indicates nonhospitalized; dark gray with solid line indicates hospitalized), from 0 to 365 days after seroconversion. The key is shared across panels D–F. S/C, signal-to-cutoff value.

terms of study design, timing, spatial scale, and testing strategies. We included large-scale serosurveys performed using assays with demonstrable heterogeneities in antibody responses, as they would be most affected by issues of spectrum bias (11).

Reconstructing time series of symptom-onset dates in the locations of selected serosurveys

As assay sensitivity is estimated as a function of time since symptom onset; the distribution of potential times since symptom onset in each study population must be known or estimated, relative to the timing of the serosurvey.

Various data sources can be used as a proxy for population exposure, including time series counts of symptom onsets, positive tests, hospitalizations, and deaths (32). We obtained publicly available time series for each serosurvey locale (Table 2) and used symptom onsets as the time metric for both assay sensitivity and epidemic time series. Where only reporting dates—but not date of symptom onset—was available (i.e., United States, Manaus, and Japan), we applied a back-calculation procedure to reconstruct time series of daily symptom onsets using the EpiNow2 software package (33) and parameter estimates for the relevant time delay distributions (34–36) (see Web Appendix 3; Web Table 3). Back-calculation was not necessary for the Italy and Spain time series, as they directly report case counts by date of

Table 2. SARS-CoV-2 Epidemic Time Series Data Sets Included From Italy, Spain, United States, Manaus (Brazil), and Japan, 2020–2021

Population	Data Type (Frequency)	Time Delay Distribution(s) Needed to Obtain Symptom Onset Time Series	Date of First Available Data Point	Spatial Resolution	Reference
Italy	Reported symptom onsets (daily)[a]	N/A	January 28, 2020	Region	Istituto Superiore di Sanità, EpiCentro ([54](#), [55](#))
Spain	Reported symptom onsets (daily)	N/A	January 1, 2020	Province	Gobierno de España, Centro Nacional de Epidemiología ([56](#))
United States	Reported cases and deaths (daily)	Case/death report to symptom onset	January 21, 2020	State	*New York Times* ([57](#))
Manaus, Brazil	Reported hospitalizations (daily)	Hospitalization report to symptom onset	March 16, 2020	Single city	Fundação de Vigilância em Saúde do Amazonas—FVS/AM ([58](#), [59](#))
Japan	Reported cases and deaths (daily)	Case/death report to symptom onset	January 16, 2020	Prefecture	National-level data sets from the Ministry of Health, Labour, and Welfare ([60](#), [61](#)) Prefectural and prefectural-level data sets from prefectural ministries of health ([62–66](#))

Abbreviations: N/A, not available; SARS-CoV-2, severe acute respiratory syndrome coronavirus 2.
[a] Region-level data are of positive tests and are available from February 24, 2020, onward.

symptom onset. We also shifted the (reconstructed) time series of symptom onsets forward by 21 days to account for the time between symptom onset and seroconversion.

Subnational time series in Italy, Spain, and Japan were generally congruent to national time series during waves of infection included here, so we used a single national-level time series to represent recency of infection for these serosurveys (Web Figures 1–3). Assay-specific seroprevalence data in the United States were available only at the census-division level, so we aggregated state-level time series to the census division using weights derived from the number of samples tested by state and by survey round (Web Figure 4). As available, we compared results of symptom onset reconstruction from multiple sources of data (Web Figures 5–6).

Joint framework for obtaining estimates of cumulative incidence from seroprevalence data

For each serosurvey, we first calculated a single time-varying assay sensitivity, obtained as the average of the severity-specific, time-varying sensitivities, weighted by the expected distribution of disease severities among the serosurvey population. We considered the age distribution of participants in the serosurvey and combined this with published estimates on age-specific weights for the expected proportions of asymptomatic, nonhospitalized, and hospitalized infections (Web Tables 4–8, Web Figure 7, Web Appendix 4). Although a degree of variation in population age structure exists across the included serosurveys, the resulting distribution of severities was, on average, 5% hospitalized (severe), 45% symptomatic and not hospitalized, and 50% asymptomatic.

To obtain an estimate of the expected sensitivity of the assay at the time of a serosurvey, we calculated the dot product of the severity-weighted time-varying assay sensitivity and the difference between the reconstructed time series of symptom onsets and the date of the serosurvey. Using the posterior distribution of this single weighted sensitivity that accounts for both severity and time, along with the manufacturer-reported point estimates of specificity for each assay (Web Table 2), we obtained estimates of cumulative incidence and 95% credible intervals using the Rogan-Gladen estimator ([3](#)) or a binomial model ([4](#)); a multinomial model ([37](#), [38](#)) was used for the 2-assay scenario (see Web Appendix 5–6). We used the R statistical software (version 3.5.3; R Foundation for Statistical Computing, Vienna, Austria), EpiNow2 R package (version 1.2.1) ([33](#)), and the Stan programming language (versions 2.19.3 and 2.21.2; Stan Development Team, https://mc-stan.org) for all analyses.

RESULTS

Kinetics of antibody responses and time-varying, severity-specific assay sensitivity

Across each of the 3 assays included here (ARCHITECT, Abbott Core Laboratory, Abbott Park, Illinois; Elecsys, Roche Diagnostics, Indianapolis, Indiana; and VITROS

IgG, Ortho Clinical Diagnostics, Raritan, New Jersey), average antibody responses in hospitalized individuals were consistently higher than those in nonhospitalized individuals, and thus sensitivity estimates were higher in this group (Figure 2). Antibody responses in nonhospitalized individuals were strikingly heterogeneous: Some individuals had high responses on par with hospitalized individuals, while others had distinctly lower responses. Antibody responses and estimated sensitivities on the Abbott ARCHITECT assay and, to a lesser extent, the Ortho VITROS IgG assay decayed over time, while they remained stable on the Roche Elecsys assay. Additional time points tested suggest that these trends persisted over subsequent months (Web Figure 8). Although limited by a small sample size in our study, assay sensitivity for asymptomatic individuals may be substantially lower than that for nonhospitalized, symptomatic individuals (Web Figure 9). We identified similar antibody waning rates on the Abbott ARCHITECT assay in longitudinal samples from the blood-donor population in Manaus used for SARS-CoV-2 serosurveillance (Web Figure 10).

Since the serosurveys in Japan performed parallel testing on the Abbott ARCHITECT and Roche Elecsys assays, we jointly modeled the probability of testing positive on both assays, given prior infection. We found that this was highest in the earliest times since infection; the probability of testing negative on Abbott and positive on Roche increased over time, consistent with relatively rapid declines in sensitivity over time on the Abbott assay and consistently high sensitivity of the Roche assay (Web Figure 11). Parameter values for all fitted antibody kinetics models are provided in Web Tables 9–11.

Overall impacts of serosurvey timing and demography on expected assay sensitivity

Timings of serosurveys relative to the local epidemic curve varied. In some settings, serosurveys were conducted a few months after the first peak, while others were during or after periods of ongoing transmission. Figure 3 shows reconstructed daily numbers of symptom onsets relative to the timing of each serosurvey locale. These are based on the reported time series identified in Table 2 and delay distributions identified in Web Table 3.

Estimates of expected assay sensitivity that account for local epidemic recency, antibody waning, and disease severity differed considerably from manufacturer-reported sensitivity values (Table 3). Expected sensitivity was lower when surveys were performed in locations where infections occurred longer ago, particularly for serosurveys using the Abbott assay. The serosurvey in Italy, the serosurvey rounds in Spain, and the June 2020 round of the serosurvey in Manaus were all conducted at similarly recent times relative to their local epidemics, resulting in similar expected sensitivities of around 70% based on the 2-severity-group model. In contrast, serosurveys conducted longer ago relative to their local epidemic had lower expected sensitivities (e.g., the estimate was as low as 45% for the December 2020 round of the serosurvey in Manaus). Expected sensitivity was also strongly influenced by our choice of model, and in particular

whether asymptomatic individuals were included with other nonhospitalized individuals or classified in a separate group (Web Figure 12).

Cumulative incidence estimates and degree of potential spectrum bias by survey

Italy. The raw national seroprevalence result of this population-based serosurvey, conducted between May 25 and July 15, 2020, was 2.5% using the Abbott ARCHITECT assay. Based on our 2-severity-group model, we estimated cumulative incidence to be 3.0% (95% credible interval (CrI): 2.7%, 3.4%). Based on our 3-severity-group model, cumulative incidence increased to 3.7% (95% CrI: 3.0%, 4.7%). As identified in the original serosurvey report, northern regions of the country were particularly affected during the first wave of infection (Web Figure 13A). As we set the weighted assay sensitivities to be equal across regions, the ratio of cumulative incidence to raw seroprevalence scaled with raw seroprevalence: In the Lombardy region (orange on Web Figure 13A), which had the highest raw seroprevalence at 7.5% in this survey, cumulative incidence was estimated to be 1.35-fold greater (95% CrI: 1.20, 1.55) than reported (Figure 4A; Web Figure 14). Ratios below 1 represent regions with extremely low raw seroprevalence, accounting for expected test performance (i.e., false positive results due to imperfect specificity).

Spain. The raw national seroprevalence results for this population-based serosurvey, conducted in 2 rounds, were 5.0% (round 1: April 27 through May 11, 2020) and 5.2% (round 2: May 18 through June 1, 2020), using a rapid serological test, and 4.6% (round 1) and 4.5% (round 2) using the Abbott ARCHITECT assay. Point estimates of cumulative incidence were generally consistent within provinces between rounds (Web Figure 13B; Web Figure 15), which may be explained by their close temporal spacing (early May and late May 2020). Based on our 2-severity-group model with the Abbott ARCHITECT data, we estimated cumulative incidence to be 5.8% (95% CrI: 5.2%, 6.5%) in round 1 and 5.7% (95% CrI: 5.2%, 6.5%) in round 2. The ratio of cumulative incidence to raw seroprevalence within a province and serosurvey was similar to in Italy, reaching a high of 1.35-fold increase (95% CrI: 1.21, 1.54) over the reported value in the Cuenca province (dark orange on Web Figure 13B) (Figure 4B–C). For additional context, the cumulative incidence estimates in round 2 here, using the 3-severity-group model, were as high as the raw seroprevalence measured (using a rapid test) during round 4 of the survey (7.1%), which was conducted from November 16 to 29, 2020 (39).

United States. The first 4 rounds of the US Centers for Disease Control and Prevention Nationwide Commercial Laboratory Seroprevalence Survey were conducted between July and September 2020, and tests were performed on multiple serological assay platforms at the census-division level (Web Figures 16–19) (28, 40). Point estimates of cumulative incidence at the census-division level from round 1 and round 4 using our 2-severity-group model are provided in Web Figure 13C, and estimates from the other rounds
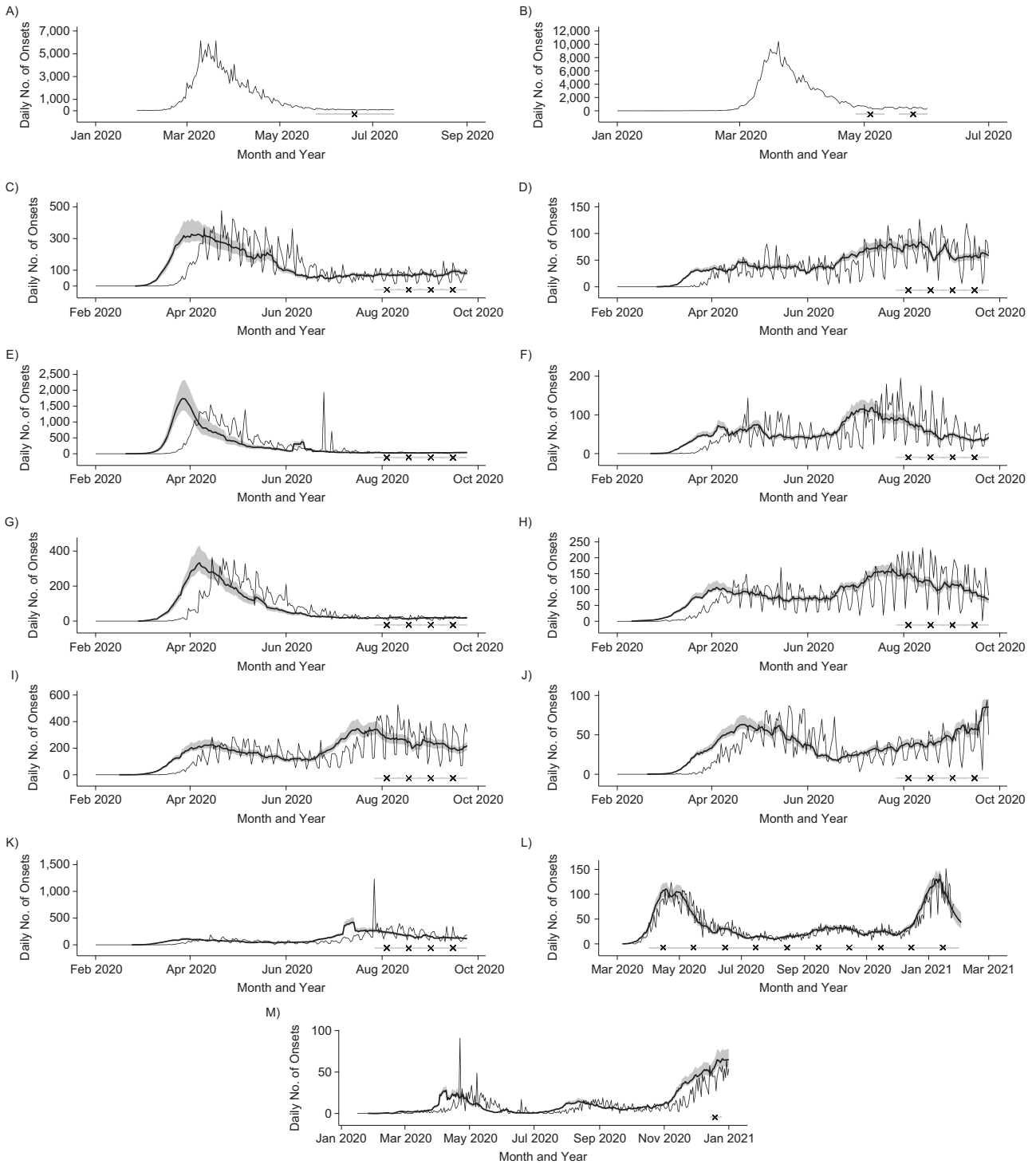
Figure 3. Reported epidemic time series from serosurvey locales, reconstructed symptom onsets, and serosurvey timing. Serosurvey dates are shown by the light gray bar (range) and black × symbol (midpoint) on the bottom of each panel. For reconstructed symptom onset curves, reported data are shown as the thin curve, and posterior median estimates and 95% credible intervals are shown in the thick curve and shaded regions. A) Reported daily symptom onsets in Italy, January to July 2020. B) Reported daily symptom onsets in Spain, January to June 2020. Daily symptom onsets by census division in the United States, reconstructed from death reports, February to September 2020, according to census division: C) East North Central, D) East South Central, E) Middle Atlantic, F) Mountain, G) New England, H) Pacific, I) South Atlantic and Puerto Rico, J) West North Central, and K) West South Central. L) Daily symptom onsets in Manaus, Brazil, reconstructed from hospitalization reports, March 2020 to January 2021. M) Daily symptom onsets in Japan, reconstructed from death reports, January to December 2020. Reconstructed symptom onsets from death reports precede deaths by approximately 3 weeks, while reconstructed symptom onsets from hospitalization reports precede hospitalizations by approximately 10 days.

Table 3. Comparison of Manufacturer-Reported Assay Sensitivity and Expected Sensitivity for Selected Rounds of Each SARS-CoV-2 Serosurvey, and the Timing of the Serosurvey Relative to the Local Epidemic, 2020–2021

Serosurvey and Round	Assay and Manufacturer-Reported Sensitivity[a]	Expected Sensitivity, 2 Severity Groups		Expected Sensitivity, 3 Severity Groups		Days Before Serosurvey of the Xth Percentile of Cumulative Symptom Onsets Prior to Serosurvey[b]				
		Posterior Mean	95% CrI	Posterior Mean	95% CrI	X = 10	X = 25	X = 50	X = 75	X = 90
Italy	100% (Abbott)	0.7072	0.6169, 0.7933	0.5672	0.4504, 0.7133	57	74	89	99	106
Spain, round 1	100% (Abbott)	0.7377	0.6520, 0.8176	0.6056	0.4853, 0.7432	20	32	42	49	54
Spain, round 2	100% (Abbott)	0.7243	0.6367, 0.8069	0.5863	0.4659, 0.7277	38	51	62	70	75
US Middle Atlantic census division, round 1	99.5% (Roche)	0.9012	0.8471, 0.9402	0.8829	0.8111, 0.9372	64	100	120	130	135
US Middle Atlantic census division, round 4	99.5% (Roche)	0.9056	0.8513, 0.9441	0.8882	0.8171, 0.9407	99	140	162	172	177
US New England census division, round 1	100% (Abbott)	0.6892	0.5959, 0.7775	0.5363	0.4138, 0.6901	61	87	107	120	129
US New England census division, round 4	100% (Abbott)	0.6376	0.5444, 0.7239	0.4834	0.3641, 0.6364	84	125	148	162	171
Manaus, June 2020	100% (Abbott)	0.7245	0.6351, 0.8074	0.5652	0.4302, 0.7208	18	34	48	61	70
Manaus, December 2020	100% (Abbott)	0.4561	0.3705, 0.5412	0.3358	0.2334, 0.4666	37	86	203	234	248
Japan	100% (Abbott)[c]	0.4931[e]	0.4233, 0.5637	0.4026[e]	0.3242, 0.5017	7	18	54	205	251
	99.5% (Roche)[d]	0.5409[c]	0.4660, 0.6127	0.4475[c]	0.3568, 0.5541					
		0.9053[d]	0.8529, 0.9433	0.8901[d]	0.8248, 0.9398					

Abbreviations: CrI, credible interval; SARS-CoV-2, severe acute respiratory syndrome coronavirus 2.

a Abbott (Abbott Park, Illinois) ARCHITECT; Roche (Indianapolis, Indiana) Elecsys.

b The rightmost 5 columns represent percentiles, in days before serosurvey. For example, in Italy, 10% of all symptom onsets occurring prior to the serosurvey occurred within the 57 days before the serosurvey, and 90% of all symptom onsets occurring prior to the serosurvey occurred within the 106 days before the serosurvey.

c Sensitivity is defined as the probability of testing positive on the Abbott assay, given infection (from a univariate model).

d Sensitivity is defined as the probability of testing positive on the Roche assay, given infection (from a univariate model).

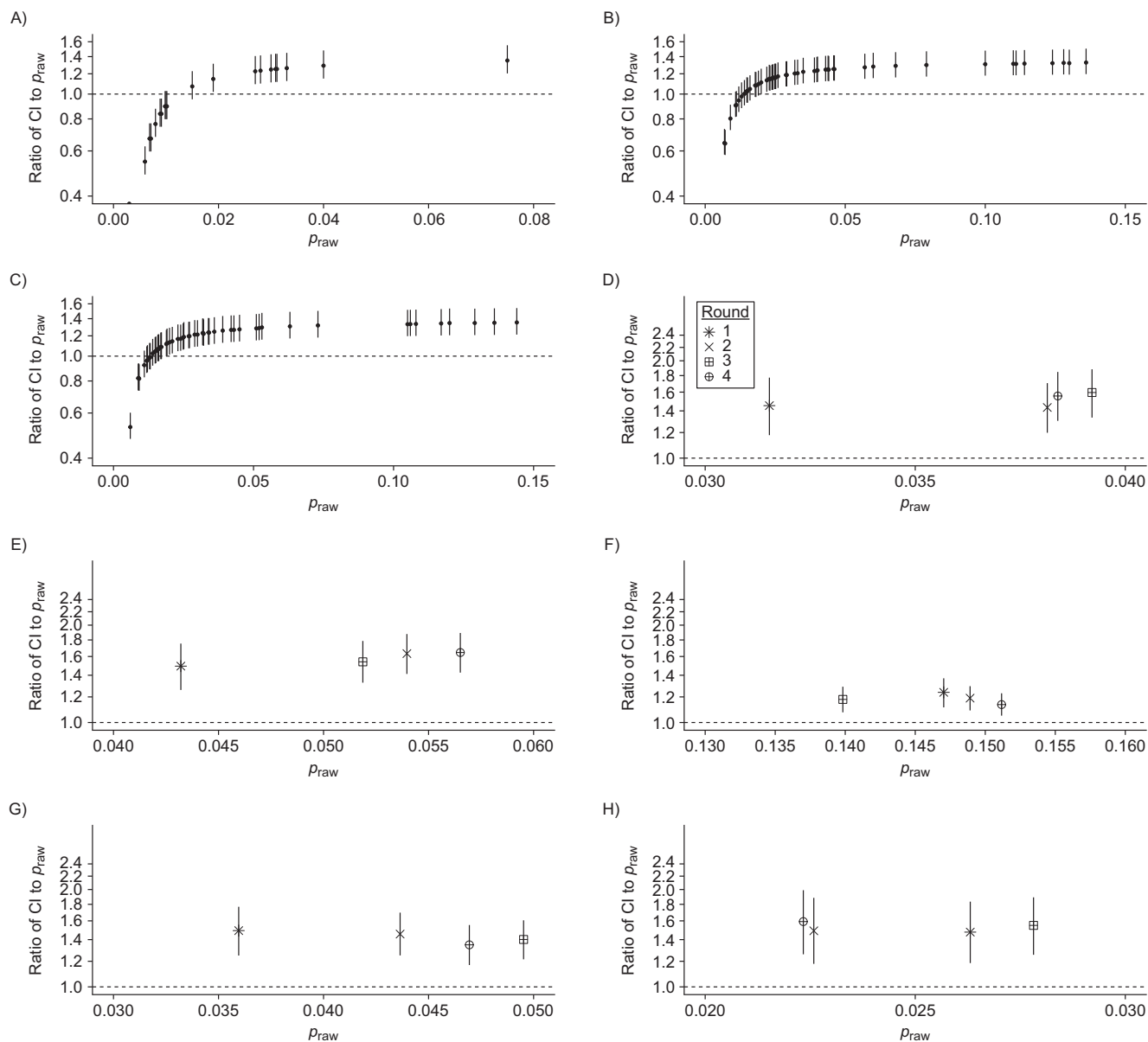e Sensitivity is defined as the probability of testing positive on both assays, given infection.

Figure 4 Continues

are available in Web Figure 20. Compared with the raw seroprevalence results, cumulative incidence estimates were up to 2-fold greater (Figure 4D–L; Web Figures 21–22). Aggregation of data from multiple serological assay platforms complicates interpretation of the raw seroprevalence results. For instance, in the Mountain census division, which comprises 8 states, all 3 assays were used; without further information, it is not possible to know which states used which combinations of the 3 assays. On the other hand, all of the data from the Middle Atlantic states (New York, New Jersey, and Pennsylvania) were from the Roche Elecsys assay (which exhibited the most stable antibody responses over time of the 3 assays), and thus the biases in cumulative

incidence estimation in this census division are the lowest in the United States.

To further explore the relative effects of time and assay choice on weighted sensitivity, we simulated serosurveys at various times at the census-division level using different proportions of tests conducted on the Abbott ARCHITECT assay (i.e., decreasing responses over time), assuming that the rest of the tests were done on the Roche Elecsys assay (i.e., stable responses over time) (Web Figure 23). In general, we found that a greater proportion of tests performed on the Abbott assay led to a lower weighted sensitivity. However, even if a serosurvey was performed exclusively with the same assay, and serosurveys were conducted at the same
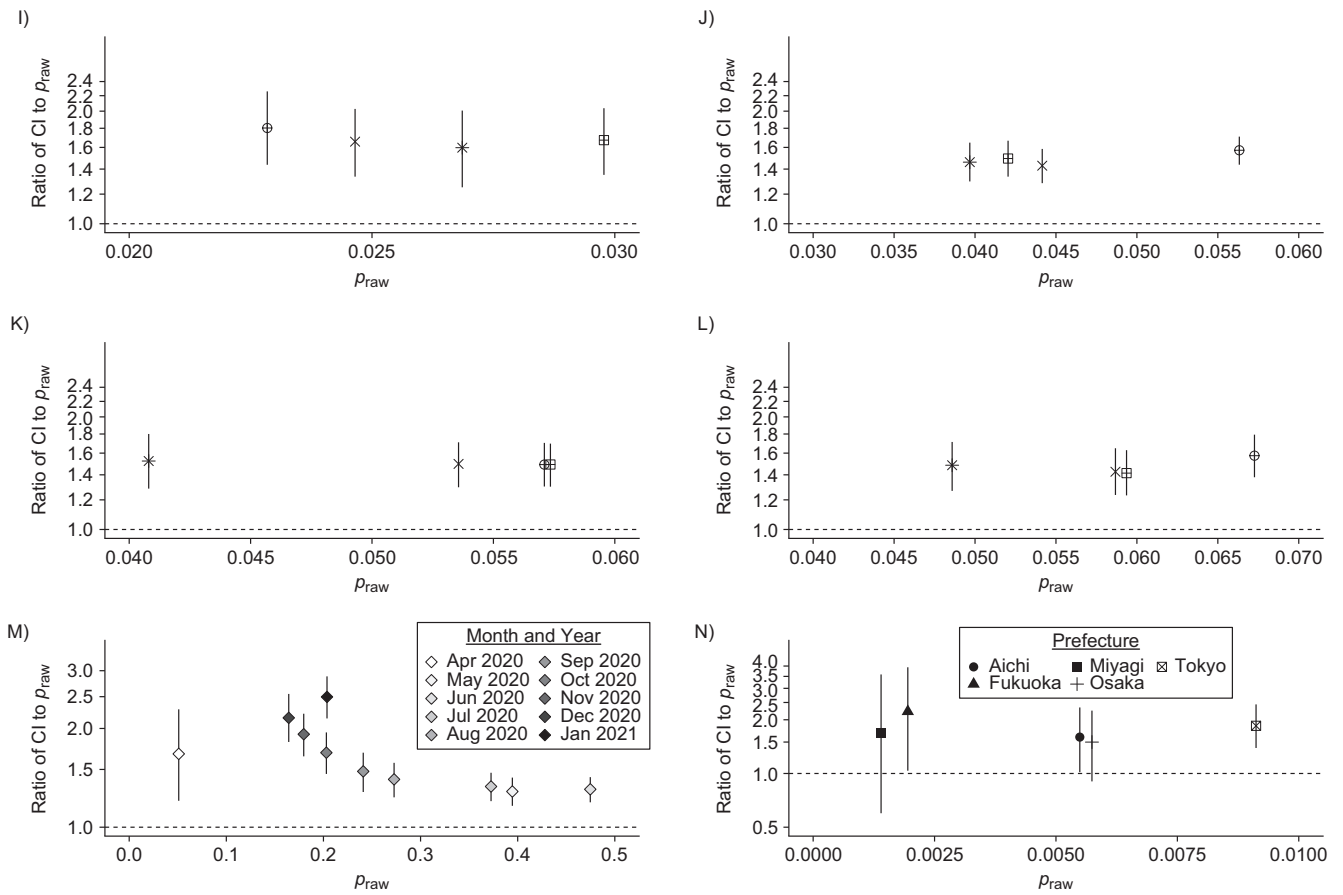
Figure 4. Relative bias in cumulative incidence estimation. For each panel, the raw seroprevalence result (p_{raw}) is shown on the *x*-axis and the ratio of the estimated cumulative incidence (CI) to raw seroprevalence is shown on the *y*-axis (median and 95% credible interval; plotted using a log2 scale). The ratio equaling 1 (i.e., no bias) is shown in the dashed horizontal line. All panels are generated under the primary scenario of classifying disease severity into 2 groups, nonhospitalized and hospitalized. A) Italy, where each point represents a region. Spain, where each point represents a province: B) round 1; C) round 2. The 9 census divisions of the United States, where the shape of the point represents the survey round (legend provided in panel D): D) East North Central, E) East South Central, F) Middle Atlantic, G) Mountain, H) New England, I) Pacific, J) South Atlantic and Puerto Rico, K) West North Central, and L) West South Central. M) Manaus, Brazil, where each point represents a month. For the United States and Manaus, Brazil, the cumulative incidence estimates are weighted by population demography and age-specific disease severity. N) Japan, where each point represents a prefecture. The scenario considered here is the case of using the results of the 2 assays.

time in all census divisions, expected assay sensitivity in the general population will differ considerably between census divisions due to the differential timings of the epidemic in the population. For example, a serosurvey conducted in February 2021 in the Middle Atlantic census division using exclusively the Abbott assay would have an expected sensitivity of 32%, while a serosurvey in the West North Central census division at the same time using the same assay would have an expected sensitivity of 59%.

Manaus, Brazil. Seroprevalence in Manaus, Brazil, has been measured monthly since April 2020 in cross-sectional samples from blood donors using the Abbott ARCHITECT assay. Manaus experienced a particularly large first wave of the SARS-CoV-2 pandemic in Spring 2020, followed by a relative trough period (Figure 3L). Both raw seroprevalence and cumulative incidence peaked in June 2020 (raw

seroprevalence of 47.5% and cumulative incidence of 61.9% (95% CrI: 56.5%, 67.5%) using the 2-severity-group model) and then declined thereafter (Web Figure 24A). Temporal changes in the ratio of cumulative incidence to raw seroprevalence echo the epidemic dynamics in Manaus, where the degree of bias increased over time from 1.28-fold (95% CrI: 1.16, 1.42) in May 2020 to 2.50-fold (95% CrI: 2.15, 2.88) in January 2021 (Figure 4M; Web Figure 25).

Japan. In the convenience sampling–based serosurveys in 5 prefectures in Japan conducted in December 2020, each sample was tested on both the Abbott ARCHITECT and the Roche Elecsys platforms (31). The raw seroprevalence values varied considerably between the univariate (single assay) and bivariate interpretations (in the latter, a sample had to be positive on both assays to be deemed a positive). We found cumulative incidence estimates to be generally

comparable between the univariate and bivariate models, but using either only Roche Elecsys or both assays led to lower uncertainty than using the Abbott ARCHITECT assay alone (Web Figure 24B). Based on our bivariate model with 2 severity groups, the ratio of cumulative incidence to raw seroprevalence ranged from 1.50-fold (95% CrI: 0.90, 2.25) in Osaka prefecture to 2.23-fold (95% CrI: 1.04, 3.94) in Fukuoka prefecture (Figure 4N; Web Figure 26). Importantly, having all samples in this serosurvey tested on 2 assays, along with validation samples also being tested on both assays, provided the opportunity to estimate the correlation between assays (37) and to incorporate this into estimation of cumulative incidence.

DISCUSSION

Differences in antibody responses as a function of disease severity and time since infection complicate inference from population-level serological data because they can substantially affect expected assay sensitivity. In the serosurveys evaluated here, we found that estimated cumulative incidence was up to 2.5-fold greater than measured raw seroprevalence. Leveraging data on the kinetics of antibody responses measured by 3 of the most widely used serological assays, we present a unified methodological framework to estimate SARS-CoV-2 cumulative incidence that accounts for these factors, and we provide a toolkit for practitioners to generate cumulative incidence estimates with either preset or custom parameter values.

We found that the degree of bias depended on the assay used, the timing of the serosurvey relative to the course of the epidemic locally, and the age distribution of the population and age-dependent probability of severe disease. The serosurvey in Italy and the 2 serosurvey rounds in Spain were conducted relatively early with respect to the local epidemic, resulting in expected sensitivities of around 70%. In the United States, the serosurveys included occurred during the first and second waves of the pandemic and used different assays in different census divisions, affecting the magnitude of the bias in estimated cumulative incidence. In the Middle Atlantic census division, the magnitude of the bias was attenuated due to the exclusive use of the Roche assay; in the New England census division, which used the Abbott assay exclusively, the magnitude of the bias was greater. In Japan, the serosurvey was conducted almost a year after the first case of COVID-19 was reported (41). While the absolute magnitudes of both raw seroprevalence and cumulative incidence were low (under 2%), expected sensitivity on the Abbott assay for this serosurvey was as low as 54%.

In Manaus, the magnitude of the bias increased continuously from 1.28-fold in May 2020 to 2.50-fold in January 2021, revealing the footprint of the first wave of the pandemic in early 2020. These results corroborate findings that cumulative incidence was likely already high prior to the subsequent resurgence of SARS-CoV-2 infection in late 2020 (16, 30). The decrease in cumulative incidence estimates after June 2020 suggest that these adjustments for severity and time may be insufficient, as cumulative incidence is monotonically increasing by definition. This discrepancy could be attributable to issues of sampling, age-patterns not adequately captured in this framework, or higher waning rates. The framework developed here provides an alternative to a previously developed approach (16). Our framework does not impose assumptions on cumulative incidence estimates monotonically increasing at each month, but rather assumes that reported case counts (in this instance, hospitalizations) are an accurate reflection of temporal trends in transmission. Our framework implicitly assumes temporal homogeneity in the case-fatality ratio, case-hospitalization ratio, and the case-reporting ratio. Known deviations from this assumption through estimation of time-varying metrics could be incorporated to improve the accuracy of estimates (e.g., potential decreases in the case-fatality ratio over time (42)).

This approach is broadly applicable beyond the assays and serosurveys included. We previously presented cohort data to estimate time-varying sensitivity of 11 additional assays (18), and numerous studies have also studied longitudinal antibody responses on an array of platforms (43–45). A key methodological development here is in providing a framework to use these data to adjust for time since infection, as informed by the local epidemic in a population of interest, allowing comparisons within and between locales. This framework incorporates setting-specific scenarios, including the availability of different types of reported epidemiologic data, population representativeness of the serosurvey and necessary adjustments for weights, spatial scale, study design, and testing strategy.

Two assays included here, the Abbott ARCHITECT and Ortho VITROS IgG, have considerable waning over the first 5 months following infection. Persistence of these trends will lead to further decreases in assay sensitivity. Over time, antibody waning will be increasingly important to account for in estimating cumulative incidence from seroprevalence data, as more individuals will have been infected longer ago and with greater variability. These considerations will be important for interpreting subsequent rounds of serosurveys included here (e.g., Spain (39) and the United States (40)) and others not included (e.g., India (46)). These considerations underscore the need for continued longitudinal follow-up of individuals with confirmed SARS-CoV-2 infection (and various strains), as antibody kinetics often follow more complex dynamics of boosting and waning over time beyond linear changes (47). Assays demonstrating more waning may be better suited for other use-cases such as identifying recent infections. An additional consideration for designing a serosurvey in places where mRNA vaccines are used is using assays measuring antibodies to nonspike proteins, which will play a role in distinguishing immune responses to infection versus vaccine-elicited immune responses to the spike protein alone.

There are a number of caveats associated with this analysis. The accuracy of this approach hinges on the accuracy of symptom onset curves reconstructed from the selected reported time series. This limitation is not unique to estimation of cumulative incidence; downstream metrics such as the time-varying reproduction number similarly rely on the robustness of these data streams over time (33, 48).

Estimation will also be sensitive to the data type chosen; for example, hospitalizations and deaths are generally more robust to temporal trends in under-ascertainment than cases, but this may be context-specific.

A key consideration is the small sample size for asymptomatically infected individuals, who potentially comprise a majority of all SARS-CoV-2 infections (49, 50). While the distinction between asymptomatic versus minimally symptomatic may be difficult to define, it is imperative to better understand the magnitude and kinetics of antibody responses in this group of individuals to better understand the extent of bias in cumulative incidence estimates. The decision to model asymptomatic individuals as their own severity group or aggregated with the other nonhospitalized individuals has a major effect on overall cumulative incidence. Our framework accounts for differences in assay sensitivity by disease severity and time but does not explicitly incorporate other potentially important sources of variation, such as age and sex, which could have additional effects on antibody responses (17, 51, 52). Last, our focus has been on sensitivity, and we do not allow for specificity to vary over time.

This work provides a broadly applicable framework incorporating individual-level immune dynamics into epidemiologic models to produce unbiased cumulative incidence estimates for a number of serosurvey-specific scenarios. The methodology has been made publicly available for broad public use. More accurate seroprevalence estimates will allow for better understanding of the proportion that has been exposed to date, and for various applications including integration into downstream mechanistic transmission models.

REFERENCES

1. Arora RK, Joseph A, Van Wyk J, et al. SeroTracker: a global SARS-CoV-2 seroprevalence dashboard. *Infect Dis.* 2021; 21(4):e75–e76.
2. Chen X, Chen Z, Azman AS, et al. Serological evidence of human infection with SARS-CoV-2: a systematic review and meta-analysis. *Global Health.* 2021;9(5):e598–e609.
3. Rogan WJ, Gladen B. Estimating prevalence from the results of a screening test. *Am J Epidemiol.* 1978;107(1):71–76.
4. Gelman A, Carpenter B. Bayesian analysis of tests with unknown specificity and sensitivity. *Appl Stat.* 2020;69(5): 1269–1283.
5. Larremore DB, Fosdick BK, Zhang S, et al. Jointly modeling prevalence, sensitivity and specificity for optimal sample allocation [preprint]. *bioRxiv.* (https://doi.org/10.1101/2020.05.23.112649). Accessed October 12, 2020.
6. Chen Y, Tong X, Li Y, et al. A comprehensive, longitudinal analysis of humoral responses specific to four recombinant antigens of SARS-CoV-2 in severe and non-severe COVID-19 patients. *PLoS Pathog.* 2020;16(9):e1008796.

7. Hu WT, Howell JC, Ozturk T, et al. Antibody profiles according to mild or severe SARS-CoV-2 infection, Atlanta, Georgia, USA, 2020. *Emerg Infect Dis.* 2020;26(12): 2974–2978.

8. Iyer AS, Jones FK, Nodoushani A, et al. Persistence and decay of human antibody responses to the receptor binding domain of SARS-CoV-2 spike protein in COVID-19 patients. *Sci Immunol.* 2020;5(52):eabe0367.

9. Ibarrondo FJ, Fulcher JA, Goodman-Meza D, et al. Rapid decay of anti-SARS-CoV-2 antibodies in persons with mild Covid-19. *N Engl J Med.* 2020;383(11):1085–1087.

10. Ransohoff DF, Feinstein AR. Problems of spectrum and bias in evaluating the efficacy of diagnostic tests. *N Engl J Med.* 1978;299(17):926–930.

11. Takahashi S, Greenhouse B, Rodríguez-Barraquer I. Are seroprevalence estimates for severe acute respiratory syndrome coronavirus 2 biased? *J Infect Dis Suppl.* 2020; 222(11):1772–1775.

12. Chen S, Flegg JA, White LJ, et al. Levels of SARS-CoV-2 population exposure are considerably higher than suggested by seroprevalence surveys [preprint]. *bioRxiv.* 2021. (http://medrxiv.org/lookup/doi/10.1101/2021.01.08.21249432). Accessed September 14, 2021.

13. Shioda K, Lau MS, Kraay AN, et al. Estimating the cumulative incidence of SARS-CoV-2 infection and the infection fatality ratio in light of waning antibodies [preprint]. *medRxiv.* 2020. (https://doi.org/10.1101/2020.11.13.20231266). Accessed September 14, 2021.

14. Perez-Saez J, Zaballa M-E, Yerly S, et al. Persistence and detection of anti-SARS-CoV-2 antibodies: immunoassay heterogeneity and implications for serosurveillance [preprint]. *bioRxiv.* 2021. (http://medrxiv.org/lookup/doi/10.1101/2021.03.16.21253710). Accessed September 14, 2021.

15. Imperial College COVID-19 Response Team. Report 34—COVID-19 infection fatality ratio estimates from seroprevalence. https://www.imperial.ac.uk/mrc-global-infectious-disease-analysis/covid-19/report-34-ifr/. Accessed April 6, 2021.

16. Buss LF, Prete CA Jr, Abrahim CMM, et al. COVID-19 herd immunity in the Brazilian Amazon [preprint]. *medRxiv.* 2020. (https://doi.org/10.1101/2020.09.16.20194787). Accessed September 14, 2021.

17. Salje H, Tran Kiem C, Lefrancq N, et al. Estimating the burden of SARS-CoV-2 in France. *Science.* 2020;369(6500): 208–211.

18. Peluso MJ, Takahashi S, Hakim J, et al. SARS-CoV-2 antibody magnitude and detectability are driven by disease severity, timing, and assay [preprint]. *medRxiv.* 2021. (https://doi.org/10.1101/2021.03.03.21251639). Accessed September 14, 2021.

19. Peluso MJ, Deitchman AN, Torres L, et al. Long-term SARS-CoV-2-specific immune and inflammatory responses across a clinically diverse cohort of individuals recovering from COVID-19 [preprint]. *medRxiv.* 2021. (https://doi.org/10.1101/2021.02.26.21252308). Accessed September 14, 2021.

20. Peluso MJ, Kelly JD, Lu S, et al. Rapid implementation of a cohort for the study of post-acute sequelae of SARS-CoV-2 infection/COVID-19 [preprint]. *medRxiv.* 2021. (https://doi.org/10.1101/2021.03.11.21252311). Accessed September 14, 2021.

21. Long Q-X, Liu B-Z, Deng H-J, et al. Antibody responses to SARS-CoV-2 in patients with COVID-19. *Nature Med.* 2020; 26(6):845–848.

22. Verity R, Okell LC, Dorigatti I, et al. Estimates of the severity of coronavirus disease 2019: a model-based analysis. *Lancet Infect Dis.* 2020;20(6):669–677.

23. Teunis PFM, van Eijkeren JCH, Ang CW, et al. Biomarker dynamics: estimating infection rates from serological data. *Stat Med.* 2012;31(20):2240–2248.

24. Istituto Nazionale di Statistica. Primi risultati dell'indagine di sieroprevalenza sul SARS-CoV-2. 2020. https://www.istat.it/it/archivio/246156. Accessed October 12, 2020.

25. Instituto de Salud Carlos III. Estudio Nacional de sero-Epidemiología de la infección por SARS-CoV-2 en España (ENECOVID): INFORME FINAL. https://portalcne.isciii.es/enecovid19/informes/informe_final.pdf. Accessed October 12, 2020.

26. Pollán M, Pérez-Gómez B, Pastor-Barriuso R, et al. Prevalence of SARS-CoV-2 in Spain (ENE-COVID): a nationwide, population-based seroepidemiological study. *Lancet (North American ed).* 2020;396(10250): 535–544.

27. Pastor-Barriuso R, Pérez-Gómez B, Hernán MA, et al. Infection fatality risk for SARS-CoV-2 in community dwelling population of Spain: nationwide seroepidemiological study. *BMJ.* 2020;371:m4509.

28. Bajema KL, Wiegand RE, Cuffe K, et al. Estimated SARS-CoV-2 seroprevalence in the US as of September 2020. *JAMA Intern Med.* 2021;181(4):450–460.

29. Buss LF, Prete CA Jr, Abrahim CMM, et al. Three-quarters attack rate of SARS-CoV-2 in the Brazilian Amazon during a largely unmitigated epidemic. *Science.* 2021;371(6526): 288–292.

30. Sabino EC, Buss LF, Carvalho MPS, et al. Resurgence of COVID-19 in Manaus, Brazil, despite high seroprevalence. *Lancet.* 2021;397(10273):452–455.

31. Ministry of Health, Labour and Welfare of Japan. Kōtai hoyū chōsa (dai 2-kai) sokuhō kekka [in Japanese]. https://www.mhlw.go.jp/content/000734482.pdf. Accessed April 1, 2021.

32. Reproduction number (R) and growth rate (r) of the COVID-19 epidemic in the UK. https://royalsociety.org/-/media/policy/projects/set-c/set-covid-19-R-estimates.pdf. Accessed September 14, 2021.

33. EpiNow2: estimate real-time case counts and time-varying epidemiological parameters. https://epiforecasts.io/EpiNow2/index.html. Accessed April 1, 2021.

34. Nishiura H. Time variations in the transmissibility of pandemic influenza in Prussia, Germany, from 1918–19. *Theor Biol Med Model.* 2007;4(1):20.

35. Bi Q, Wu Y, Mei S, et al. Epidemiology and transmission of COVID-19 in 391 cases and 1286 of their close contacts in Shenzhen, China: a retrospective cohort study. *Lancet Infect Dis.* 2020;20(8):911–919.

36. Linton NM, Kobayashi T, Yang Y, et al. Incubation period and other epidemiological characteristics of 2019 novel coronavirus infections with right truncation: a statistical analysis of publicly available case data. *J Clin Med.* 2020; 9(2):538.

37. Gardner IA, Stryhn H, Lind P. Conditional dependence between tests affects the diagnosis and surveillance of animal diseases. *Prev Vet Med.* 2000;45(1–2):107–122.

38. Appa A, Takahashi S, Rodriguez-Barraquer I, et al. Universal PCR and antibody testing demonstrate little to no transmission of SARS-CoV-2 in a rural community [preprint]. *medRxiv.* 2020. (https://doi.org/10.1101/2020.08.15.20175786). Accessed September 14, 2021.

39. Instituto de Salud Carlos III. Estudio Nacional de sero-Epidemiología de la infección por SARS-CoV-2 en España (ENECOVID): CUARTA RONDA. https://portalcne.isciii.es/enecovid19/informes/informe_cuarta_ronda.pdf. Accessed April 5, 2021.

40. Centers for Disease Control and Prevention. COVID Data Tracker. https://covid.cdc.gov/covid-data-tracker/#national-lab. Accessed April 2, 2021.

41. Ministry of Health, Labour and Welfare of Japan. Shingata koronauirusu ni kanren shita haien no kanja no hassei ni tsuite (1 reime) [in Japanese]. https://www.mhlw.go.jp/stf/newpage_08906.html. Accessed June 1, 2021.

42. Cheng C, Zhou H, Weiss JC, et al. Unpacking the drop in COVID-19 case fatality rates: a study of national and Florida line-level data [preprint]. *arXiv.* 2020. (http://arxiv.org/abs/2012.04825). Accessed September 14, 2021.

43. Ainsworth M, Andersson M, Auckland K, et al. Performance characteristics of five immunoassays for SARS-CoV-2: a head-to-head benchmark comparison. *Lancet Infect Dis.* 2020;20(12):1390–1400.

44. Di Germanio C, Simmons G, Kelly K, et al. SARS-CoV-2 Antibody persistence in COVID-19 convalescent plasma donors [preprint]. *medRxiv.* 2021. https://www.medrxiv.org/content/10.1101/2021.09.09.21263139v1.abstract. Accessed April 5, 2021.

45. Muecksch F, Wise H, Batchelor B, et al. Longitudinal serological analysis and neutralizing antibody levels in coronavirus disease 2019 convalescent patients. *J Infect Dis.* 2021;223(3):389–398.

46. Murhekar MV, Bhatnagar T, Selvaraju S, et al. SARS-CoV-2 antibody seroprevalence in India, August–September, 2020: findings from the second nationwide household serosurvey. *Lancet Glob Health.* 2021;9(3):e257–e266.

47. Huang AT, Garcia-Carreras B, Hitchings MDT, et al. A systematic review of antibody mediated immunity to coronaviruses: kinetics, correlates of protection, and association with severity. *Nat Commun.* 2020;11(1):4704.

48. Gostic KM, McGough L, Baskerville EB, et al. Practical considerations for measuring the effective reproductive number, Rt. *PLoS Compute Biol.* 2020;16(12):e1008409.

49. Davies NG, Klepac P, Liu Y, et al. Age-dependent effects in the transmission and control of COVID-19 epidemics. *Nature Med.* 2020;26(8):1205–1211.

50. Meyerowitz EA, Richterman A, Bogoch II, et al. Towards an accurate and systematic characterisation of persistently asymptomatic infection with SARS-CoV-2. *Lancet Infect Dis.* 2021;21(6):e163–e169.

51. Takahashi T, Wong P, Ellingson M, et al. Sex differences in immune responses to SARS-CoV-2 that underlie disease outcomes [preprint]. *medRxiv.* 2020. (https://doi.org/10.1101/2020.06.06.20123414). Accessed September 14, 2021.

52. Klein SL, Pekosz A, Park H-S, et al. Sex, age, and hospitalization drive antibody responses in a COVID-19 convalescent plasma donor population. *Clin Res.* 2020;130(11):6141–6150.

53. Istituto Nazionale di Statistica. Primi risultati dell'indagine di sieroprevalenza sul SARS-CoV-2; https://www.istat.it/it/files//2020/08/ReportPrimiRisultatiIndagineSiero.pdf. Accessed April 1, 2021.

54. EpiCentro. Sorveglianza integrata COVID-19: i principali dati nazionali. https://www.epicentro.iss.it/coronavirus/sars-cov-2-sorveglianza-dati. Accessed April 6, 2021.

55. Dati COVID-19 Italia. Github. https://github.com/pcm-dpc/COVID-19. Accessed April 6, 2021.

56. Instituto de Salud Carlos III. COVID-19 en España. https://cnecovid.isciii.es/covid19/resources/casos_diagnostico_provincia.csv. Accessed December 27, 2022.

57. Covid-19-data. Github. https://github.com/nytimes/covid-19-data. Accessed April 1, 2021.

58. Transparência COVID-19: séries temporais COVID-19 no Amazonas. https://www.fvs.am.gov.br/indicadorSalaSituacao_view/69/2. Accessed April 1, 2021.

59. Séries temporais COVID-19 Amazonas. https://public.tableau.com/profile/astec.sass#!/vizhome/Subnotificao/HospMun. Accessed April 6, 2021.

60. Ministry of Health, Labour and Welfare of Japan. Open data. https://www.mhlw.go.jp/stf/covid-19/open-data_english.html. Accessed April 6, 2021.

61. Office for COVID-19 and Other Emerging Infectious Disease Control, Cabinet Secretariat, Government of Japan. Shingata koronauirusukansenshō taisaku [in Japanese]. https://corona.go.jp/dashboard/. Accessed April 6, 2021.

62. Tokyo Metropolitan Government COVID-19 Information Website [in Japanese]. https://stopcovid19.metro.tokyo.lg.jp/. Accessed April 6, 2021.

63. Osaka Prefecture COVID-19 Task Force website: Number of people testing positive. https://covid19-osaka.info/data/summary.csv. Accessed April 6, 2021.

64. Miyagi ken'nai no saishin kansen dōkō [in Japanese]. https://www.pref.miyagi.jp/site/covid-19/02.html. Accessed April 6, 2021.

65. Aichi ken shingata koronauirusukansenshō taisaku saito [in Japanese]. https://stopcovid19.code4.nagoya/. Accessed April 6, 2021.

66. Fukuoka ken shingata koronauirusukansenshō yōsei-sha happyō jōhō—jichitai ōpundēta no CKAN [in Japanese]. https://ckan.open-governmentdata.org/dataset/401000_pref_fukuoka_covid19_patients. Accessed April 6, 2021.